HHS Public Access

Author manuscript

Nat Nanotechnol. Author manuscript; available in PMC 2019 September 25.

Published in final edited form as:

Nat Nanotechnol. 2019 June ; 14(6): 616–622. doi:10.1038/s41565-019-0406-1.

FDA-approved ferumoxytol displays anti-leukaemia efficacy against cells with low ferroportin levels

Vicenta Trujillo-Alonso[†,1], **Edwin C. Pratt**[†,2,3], **Hongliang Zong**[1], **Andres Lara-Martinez**[1], **Charalambos Kaittanis**[3], **Mohamed O. Rabie**[1], **Valerie Longo**[4], **Michael W. Becker**[6], **Gail J. Roboz**[1], **Jan Grimm**[*,2,3,5,7], and **Monica L. Guzman**[*,1,2]

[1]Division of Hematology/Oncology, Department of Medicine, Weill Cornell Medical College, New York, NY 10021, USA.

[2]Department of Pharmacology, Weill Cornell Graduate School, New York, NY 10021, USA

[3]Molecular Pharmacology Program, Memorial Sloan Kettering Cancer Center, New York, NY 10065, USA.

[4]Small-Animal Imaging Core Facility, Memorial Sloan Kettering Cancer Center, New York, NY 10065

[5]Department of Radiology, Weill Cornell Medical College, New York, NY 10021, USA.

[6]Department of Medicine, Wilmot Cancer Institute, University of Rochester Medical Center. Rochester, NY.

[7]Department of Radiology, Memorial Sloan Kettering Cancer Center, New York, NY 10065, USA.

Abstract

Acute myeloid leukaemia (AML) is a fatal disease for most patients. We have found that ferumoxytol (Feraheme®), a FDA approved iron oxide nanoparticle for iron deficiency treatment, demonstrates an anti-leukaemia effect in vitro and in vivo. Using leukaemia cell lines and primary AML patient samples, we show that low expression of the iron exporter ferroportin (FPN) results in a susceptibility of these cells by an increase in intracellular iron from ferumoxytol. The reactive oxygen species produced by free ferrous iron leads to increased oxidative stress and cell death. Ferumoxytol treatment results in a significant reduction of disease burden in a murine leukaemia model and patient-derived xenotransplants (PDX) bearing leukaemia cells with low FPN expression. Our findings show how a clinical nanoparticle considered previously largely

[*]To whom correspondence should be addressed., mlg2007@med.cornell.edu; grimmj@mskcc.org.
[†]Equal contribution

Author contributions: V.T., E.C.P., H.Z., C.K., J.G., and M.L.G. devised and conducted experiments, and wrote this manuscript. A.L-M. and M.O.R. performed experiments. M.W.B and G.J.R. discussed data, wrote manuscript. V.L. conduced injections.

Competing interests: J.G., C.K., H. Z., and M.G. have filed pending US patent application 15/759,161 and pending EU application 16845094.8 around the therapeutic use of Ferumoxytol. C.K. is currently an employee of Alnylam Pharmaceuticals.

Data availability: The data that support the plots within this paper and other findings of this study are available from the corresponding author upon reasonable request.

biologically inert could be rapidly incorporated into clinical trials for patients with leukaemia with low FPN levels.

One Sentence Summary:

Administration of the clinically approved iron oxide nanoparticle drug ferumoxytol in vitro results in an anti-leukaemia effect and in vivo extended overall survival in part due to the low expression of the iron export protein ferroportin.

Acute myeloid leukaemia (AML) is a heterogeneous blood cancer that results from an abnormal proliferation of white blood cells initiated and maintained by leukemic stem cells (LSCs). AML is the most common type of acute leukaemia in adults with poor survival rates for adults and children with an overall five-year survival rate of 27% to 65%[1,2]. Despite aggressive treatments that include bone marrow transplantation, most patients that achieve complete remission will relapse and ultimately die from their disease. Even though diverse chemotherapeutic agents have shown promise against AML, successful treatment has been hampered by (i) low therapeutic index of chemotherapeutic drugs, (ii) insufficient effect on quiescent cells such as LSCs, which give rise to and maintain disease, and (iii) off-target effects [3]. Critical to the development of an effective therapy for AML is identifying unique key dysregulated mechanisms that can be used as therapeutic targets[4]. In AML, it has been increasingly acknowledged that LSCs are a major contributor for leukaemia chemoresistance and relapse[5]. Thus, therapies that target selectively LSCs without harming normal hematopoietic stem cells (HSCs) will improve outcomes and provide fewer systemic side effects.

AML treatment has relied on induction therapy, with the gold standard clinical practice being cytarabine arabinoside (Ara-C) administered with an anthracycline. However, this and other therapies have not led to significant differences in overall survival or disease-free survival in the clinic [6]. In the preclinical space, parthenolide (PTL) and its derivatives have shown therapeutic promise as inhibitors of NF-κB for the elimination of LSCs [7]. LSCs are susceptible to PTL as they have constitutive activation of NF-κB compared to the normal HSCs. PTL administration drives leukemic cells into apoptosis by glutathione depletion. PTL showed a synergistic effect by sensitizing LSCs to drugs that generate reactive oxygen species (ROS), such as buthionine sulfoximine[8]. ROS can also be produced through the Fenton reaction when ferrous iron is present with peroxide and oxygen[9]. This ROS production natively is balanced by antioxidant production in combination with iron transport systems, such as transferrin internalization, storage by ferritin, and iron export by ferroportin (FPN), the sole known cellular exporter of iron.

Regulation of FPN has been well known from work in diseases relating to iron storage, such as hemochromatosis. Importantly, FPN is the only known mammalian iron exporter, potentially serving as a bottleneck for iron efflux, where low FPN expression results in low iron efflux and higher iron retention. Recently FPN has been found to be dysregulated in cancer, where more aggressive breast tumours are low in FPN expression. Furthermore, other cancers such as prostate, ovarian, colorectal and multiple myeloma are low in FPN expression relative to adjacent healthy tissues[10–15]. This suggests that the degree of loss of

FPN expression could have a potential diagnostic and prognostic value in several types of cancer. Thus, we sought to determine if the levels of expression of FPN in leukaemia using cell lines and primary samples were indeed lower than their normal bone marrow. Here we report that FPN is also expressed significantly lower across leukemic cell lines and primary AML samples including leukemic blasts, CD34+ progenitors, and phenotypically defined leukaemia stem cells compared to normal bone marrow CD34+ progenitor cells (nBM CD34+ cells). We hypothesized that low levels of FPN would result in a susceptibility of leukaemia cells to induction of ROS through the Fenton reaction by exploiting the inability of the cells to export iron.

Ferumoxytol, or Feraheme®, is an iron oxide nanoparticle clinically available for the treatment of iron deficiency anaemia in patients in the United States[16]. Ferumoxytol has been widely considered to be safe when given as a single infusion. Ferumoxytol's iron core consists of 5874 iron atoms, a mix of ferrous, Fe (II), and ferric iron, Fe (III). In the Fenton reaction, both forms of iron in the presence of peroxides can produce harmful ROS as described previously[17]. We demonstrate that leukemic cells and leukemic stem/progenitor cells are sensitive to ROS generation from ferumoxytol *in vitro* and *in vivo*. We demonstrate that ferumoxytol inhibited disease progression in a highly aggressive acute leukaemia syngeneic mouse model (blast crisis CML, driven by the dual oncogenes BCR-ABL-NUP98-HOXA9)[18,19], where ara-C cannot target LSCs as effectively as the nanoparticle ferumoxytol. In addition, we also show that ferumoxytol selectively had an anti-leukemic effect in AML-patient derived xenografts (PDX) expressing low levels of FPN. We propose that leukaemia cells with low FPN expression, are vulnerable to iron based oxidative stress and selectively sensitive to increases in ROS when administered as a nanoparticle. Importantly, normal tissue expresses higher FPN based on samples from cBioPortal[20], providing a therapeutic window for ferumoxytol administration. Together, these data suggest the potential of targeting leukaemia cells characterized by low FPN expression with oxidative ferrotherapy by administration of ferumoxytol.

Leukemic blasts and stem cells are sensitive to ferumoxytol

We and others have previously shown that leukaemia stem and progenitor cells are sensitive to ROS induction by small molecules[7,21]. Since ROS can also be produced by ferrous iron through the Fenton reaction[9] and Ferroportin (FPN) is the sole known cellular iron exporter, we hypothesized that the absence of FPN could represent an Achilles heel for these cells. Thus, we sought to evaluate FPN expression in leukaemia cell lines. Using quantitative RT-PCR we determined the mRNA expression of SLC40A1 (FPN) transcripts and found that the basal FPN expression was decreased in the majority of leukaemia cell lines in comparison with normal bone marrow CD34+ progenitor cells, with some lines showing nearly 10,000-fold lower expression (Fig. 1a, Supplementary Table 1**)**. Next, we evaluated primary AML samples, including purified CD34+ progenitor cells, and found that the mRNA expression of FPN was decreased in AML blasts and CD34+ progenitor cells (Fig. 1b, Supplementary Table. 2). We further interrogated the FPN protein levels in leukaemia cell lines and AML patient samples using flow cytometry (Fig. 1c-e). We found that most cell lines evaluated were low (16 out of 19) (Fig. 1d). Importantly, in primary AML samples, we found that FPN protein levels were significantly lower in the progenitor (CD34+) and stem (CD34+CD38-)

cell populations compared to leukemic blasts (Fig. 1e). Together, FPN mRNA and protein expression in the majority of leukaemia cell lines and primary AML samples suggest a phenotype of aberrant iron export.

Based on the low FPN expression, we next hypothesized that FPN-low cells would retain more iron and thus demonstrate a higher vulnerability to ROS with increased cell death. Iron uptake, storage and excretion are well regulated, however administration of iron in the form of the nanoparticle ferumoxytol provides an alternate uptake route. We observed by ICP-MS a modest but significant increase in iron content per mg of protein for FPN-low but no significant difference in the intracellular iron content in FPN-high cells when they were treated for 24 hours (Fig. 1f). In addition, FPN-low cells showed a significant reduction in viability 48 hours post-exposure to ferumoxytol with little to no effect on ferumoxytol high cell lines (Fig. 1g). Primary AML samples showed a similar effect at 24 hours post exposure (Supplementary Fig. 4). Human AML cell lines were found to all take up Cy5.5 labelled ferumoxytol at a high level (Supplementary Fig. 5a) and were tested for the phagocytic marker CD68 to determine any difference in uptake. We found that all cells expressed the marker suggesting that cell viability is not likely tied to the capacity of cells to phagocytize (Supplementary Fig. 5b). We next evaluated heme oxygenase-1 (HMOX1) mRNA expression as a measure of antioxidant defence activity when free iron is available. Importantly, we observed that in the FPN-low cell lines UKE-1 and KCL22 levels of HMOX1 mRNA were not significantly elevated while the MV411 cell line (FPN-low) was highly upregulated for HMOX1 (pink dot in Fig. 1h) when compared with untreated cells. Similarly, levels of GCLC mRNA were unchanged except for the same cell line, MV411, which was also elevated in mRNA expression (Fig. 1h). Expression of SLC7A11, the cystine glutamate antiporter, was also significantly upregulated in FPN-low cell lines with ferumoxytol administration. The cell line MV411 overall was the most sensitive to ferumoxytol administration in terms of cell viability and stress gene response respectively (Fig. 1g and Fig. 1h), suggesting that these cells are vulnerable to ROS accumulation driven by ferumoxytol. Additional gene expression levels relating to iron management, antioxidant production, and inflammation were also evaluated for the leukaemia cell lines and provided in Supplementary Figs. 6–8. mRNA inflammation markers IL1b, IL6, and TNFα revealed no significant increase upon ferumoxytol administration by RT-PCR (Supplementary Fig. 7). Principle component analysis (Supplementary Fig. 8**)** revealed that increases in HMOX are anticorrelated with SLC40A1 (FPN) with antioxidant genes being the strongest contributors to each principle component. Measuring cytosolic and mitochondrial ROS at 24 h and 48 h post ferumoxytol administration (Fig. 1i) confirmed FPN-low cell lines were most affected, and the greatest increases in either cytosolic or mitochondrial ROS (green and pink dots in Fig. 1g), correspond with the lowest viability cell lines. Flow cytometry fluorescence intensity plots in Supplementary Fig. 9 show the degree of ROS shift. Protection of FPN-low cell lines against ROS using the antioxidant N-acetyl cysteine confirmed oxidation by ferumoxytol contributes to cell stress and reduced viability (Supplementary Fig. 10). Measured secreted cytokines IL1b, IL6, and TNFα by flow had below detection limit levels for the AML cell lines tested and no significant increases were observed after ferumoxytol administration for 24h (Supplementary Figure 11) in line with the lack of cytokine activity by RTqPCR.

Ferumoxytol as an anti-leukemic therapy

In searching for leukaemia mouse models to evaluate the *in vivo* effect of ferumoxytol, we mined the microarray data of the blast crisis leukaemia (bcCML) model that consists of cooperative oncogenes BCR-ABL(GFP) and NUP98-HOXA9(YFP) [18,19] and found that bcCML cells (GFP+YFP+) also expressed low SLC40A1 (FPN) when compared with their normal counterparts (GFP-YFP-). This acute leukaemia model has similar target organs, aggressiveness, and refractory behaviour to chemotherapeutics as human AML. We tested the effect of ferumoxytol, and used the standard of care drug for AML, cytarabine (Ara-C) as a control. C57BL/6 female mice were transplanted with leukemic cells bearing BCR-ABL (GFP)/NUP98-HOXA9 (YFP) oncogenes[18]. Mice were bled and monitored for the percentage of leukemic blasts in peripheral blood (PB) and randomized into four different cohorts (n=7) when the blast burden in PB exceeded 0.1 %. Cohorts were administered either saline, Ara-C (40 mg/kg), or ferumoxytol low at 3 mg/kg or high at 6 mg/kg. The ferumoxytol dosages represent sub-clinical therapeutic doses for anaemia (7.3 mg/kg). Ara-C was administered by intraperitoneal injection (IP) and saline and ferumoxytol were administered intravenously (IV) twice a week as indicated in Fig. 2a. The burden of leukemic blasts was monitored every week until the onset of morbidity, at which all of the cohorts were sacrificed and evaluated for tumour burden in PB, bone marrow (BM) and spleen (SPL). In comparison with saline control group there was a significant reduction of the percentage of leukemic blasts populations in PB, BM, and SPL of mice only treated with ferumoxytol 6 mg/kg (Fig. 2b-e). Splenomegaly is a feature of blast infiltration and disease progression. We found that ferumoxytol radiolabelled with the positron emission tomography radiotracer ^{89}Zr could identify SPL and liver margins for facile quantification of SPL volume (Supplementary Fig. 12a). We found the SPL weight of animals treated with ferumoxytol 6 mg/kg was overall lower as shown by the lower SPL index (spleen weight / total body weight) (Fig. 2f), indicating decreased disease burden. These data demonstrate that ferumoxytol at 6 mg/kg was able to induce an anti-leukemic effect in PB, BM, and SPL.

Next, we evaluated the effect of ferumoxytol in overall survival of the mice via IP. Mice were treated with saline or ferumoxytol at 6 mg/kg three times a week, monitoring PB burden weekly until death (Fig 2g). ferumoxytol clearly and significantly reduced the leukemic blast burden through 21 days in PB (Fig. 2h) and had a significant increase in median survival time (25 days ferumoxytol 6mg/kg, 17 days saline) (Fig. 2i). A similar survivability study with ^{89}Zr-ferumoxytol confirmed the increase in median survivability (Supplementary Fig. 13). These findings demonstrate an anti-leukaemia effect with ferumoxytol administration alone and prolonged overall survival. Moreover, these data suggested that ferumoxytol can be a potential therapeutic against leukaemia cells and be tolerated by two different routes of administration.

Patient derived xenografts respond to ferumoxytol administration

With the observed therapeutic effect *in vivo* using the murine bcCML model, we next aimed to determine the therapeutic efficacy of ferumoxytol in AML-PDX using human primary AML cells with either FPN-high or -low expression (mRNA expression relative to nBM CD34+ cells). Established AML-PDXs were treated twice a week (Fig. 3a), and FPN-low

AML-PDXs in three different AML-PDXs showed a reduction in burden (Fig. 3b, Supplementary Fig. 14). In contrast, the FPN-high AML-PDX was unaffected. Importantly, normal hematopoietic cells, established with CD34+ cord blood (CB) and with high FPN levels remained unaffected during ferumoxytol administration. In summary, ferumoxytol selectively induced an anti-leukemic effect in FPN-low AML-PDXs without affecting FPN-high AML-PDXs or CB.

Since ferumoxytol consists of two iron oxidation states capable of undergoing the Fenton reaction, we sought to determine the native oxidative capacity of ferumoxytol in human cells from FPN-low expression AML-PDXs. Heme oxygenase-1 (HMOX1) expression is a measure of antioxidant defence activity when free iron is available, thus HMOX1 activity upon ferumoxytol administration was used as a readout of cellular oxidative stress. We detected in patient samples that ferumoxytol treatment resulted in a 2- to 6-fold increase in HMOX1 transcript levels (Fig. 3c), suggesting that ferumoxytol increases the levels of ROS in these cells. Further cell-free tests for peroxidase activity and ROS generation were done with ferumoxytol (Supplementary Figs. 15–17). Peroxidase and ROS activity rates were in a manner consistent of an enzymatic or catalytic process requiring ferumoxytol and exceeded ROS production of $FeCl_3$ after 12 minutes. In the absence of exogenous iron, primary AML samples expressing low FPN constitutively expressed higher HMOX1 with accumulated iron, suggesting that these cells were uniquely susceptible for further toxic ROS accumulation. The production of ROS from ferumoxytol demonstrates that ferumoxytol can fuel an oxidative overload in cells with significantly low FPN expression. As such, these findings encourage the usage of ferumoxytol as a cancer therapeutic, where ferumoxytol selectively targets leukaemia cells with low FPN. The selective toxicity of ferumoxytol is focused on AML samples with low FPN expression while normal stem cells and tissue with high FPN expression are spared. This opens a promising avenue to aid eradication of leukaemia (and potentially other tumour cells) cells with specific deficient iron export features in combination with existing standard of care therapy.

Oxidative effect of ferumoxytol on ferroportin low leukaemias

Our previous work with AML therapy has shown that PTL can inhibit NF-κB, deplete glutathione and thus induce pro-apoptotic cell death[7]. Separately, previous studies have highlighted the importance of FPN expression in identifying more aggressive cancers with poorer prognosis[22]. Here, we report the majority of leukaemia cell lines as well as primary AML patient samples are FPN-low (Figs. 1a-d). More so, FPN expression further decreased in leukemic stem and progenitor cells (Fig. 1e), revealing that the chemoresistant stem cell population that results in disease relapse could be vulnerable. We have shown that the administration of the FDA approved iron oxide nanoparticle ferumoxytol leads to significantly elevated iron content only in FPN-low leukemic cell lines (Fig. 1f), resulting in reduced viability (Fig. 1g, Supplementary Fig. 4). We found ferumoxytol to increase oxidative stress and antioxidant synthesis genes with no change in inflammation markers at 24h (Supplementary Figs. 7, 11). Ferumoxytol contains both ferrous and ferric forms of iron, which in the presence of endogenous cellular peroxide[23] can undergo the Fenton reaction[24] yielding either a hydroxide radical or a hydroperoxide radical from the ferrous and ferric forms respectively. As ferumoxytol contains both oxidation states, ferumoxytol serves as a

catalytic peroxide reactor when placed into a peroxide producing environment such as a cancer cell. Traditional atomic iron is well regulated, however ferumoxytol is a carboxymethyl dextran coated iron oxide nanoparticle containing over 5000 iron atoms and does enter the cell through endocytosis[25]. We have observed that the administration of ferumoxytol to FPN-low expressing leukaemia cell lines increases cytosolic and mitochondrial ROS (Fig. 1i) in agreement with the reduced viability observed (Fig. 1g). By administering ferumoxytol to FPN-low AML samples, the reduction in viability is driven in part by the increased iron retention driving the Fenton reaction with ferumoxytol together with the exhaustion of antioxidants by increased ROS production in FPN-low lines.

This ability to drive FPN-low AML lines to die with ferumoxytol represents a paradigm shift in cancer therapy, fortunately achieved with a FDA approved drug for anaemia. *In vivo*, using a blast crisis CML mouse model with FPN-low expression in leukemic blasts, we were able to observe the reduction of leukemic blasts in PB, BM and SPL, with a significant reduction in SPL burden (Figs. 2e and 2f) that could not be achieved with Ara-C during induction therapy. Ferumoxytol biodistribution has been shown previously, with radiolabelled ferumoxytol being found in the liver, spleen, and mesenteric lymph nodes[26]. Most importantly administration of ferumoxytol alone extends the survival of the mice (Fig. 2h, Supplementary Fig. 13). In blast crisis CML, infiltration of leukemic progenitors into the spleen and liver presents a challenge, leading to enlarged spleen and ultimately organ failure[27]. Here, ferumoxytol's biodistribution may be advantageous as IV administration results in rapid liver and spleen accumulation within 1 hour[26]. As the low FPN expression is a feature of the leukaemia cells, ferumoxytol could provide directed therapy in these organs.

Furthermore, the effectiveness of ferumoxytol against FPN-low leukaemia cells was extended to patient derived primary AML xenografts. *In vivo*, ferumoxytol administration showed a significant reduction in burden for FPN-low expressing AML-PDXs (Fig. 3b). Here, the reduction occurred in a mouse model lacking an adaptive immune system and we found a 6-fold increase in HMOX1 transcript levels from human leukemic cells obtained from AML-PDX after administering ferumoxytol, suggesting an increase in ROS in AML cells (Fig. 3c). Recent work has demonstrated anti-tumour efficacy of ferumoxytol through polarization of tumour-associated macrophages into the tumour-inhibiting M1 phenotype in a murine lung cancer model[28]. Here we show the anti-leukaemia effect with ferumoxytol is also observed in an immunocompromised system lacking functional macrophages and ferumoxytol treatment does not induce common inflammatory cytokines. As macrophage repolarization or immune stimulation does not play a significant role, the biological effect of ferumoxytol described here is entirely different and based on the expression of FPN within the cancer cells. We know from the Fenton reaction that iron in the presence of peroxide generates ROS without consuming the iron and allowing a catalytic process. More so we observed ferumoxytol produces ROS at a greater rate than free iron after 12 minutes and maintains a steady production rate. We propose that oxidative ferrotherapy is effective due to the inability of cells with low FPN expression to efficiently export the abundance of available iron in the form of ferumoxytol (Fig. 4) which generates ROS in excess of the cell antioxidant capacity. As ferumoxytol has been used widely for anaemia in patients with chronic kidney disease and recently approved for all patients with anemia[29], it is feasible to translate ferumoxytol to a therapeutic intervention for AMLs with low FPN expression.

Conclusions

The low iron export phenotype in leukaemias has provided a window for a clinical nanoparticle to exert toxic ROS stress and provide therapeutic benefit. By delivering an iron oxide nanoparticle that is internalized in a different way than molecular iron, ferumoxytol can supply a ROS source to leukaemias not governed by traditional iron regulation. Further studies will be needed to identify additional molecular features linked to the response to ferumoxytol by leukemic cells with low FPN to unravel synergistic therapeutic strategies. Combinations with existing FDA approved drugs that produce ROS may most immediately open avenues to eradicate leukaemias with a low iron export phenotype. This knowledge will help rationally combine ferumoxytol with yet to be approved drugs like PTL, that have already been reported to exhibit an anti-leukemic effect through ROS generation. Since no therapy for leukaemias with specific deficient iron export have been developed yet; it would be an important advance in the treatment of AML. More broadly these findings suggest the exploration of using nanoparticle iron against other cancers with a low iron export phenotype.

Materials and Methods

Primary samples

Primary AML samples and bone marrow from healthy donors were obtained with informed consent, abiding by ethical compliance requirements established and approved by Institutional Review Boards from Weill Cornell Medical College-New York Presbyterian Hospital and from the University of Rochester Medical Center. Primary cryopreserved AML samples were thawed and cultured as previously described [4]. Enrichment of CD34+ cells was performed using an indirect CD34 Microbead Isolation Kit (Miltenyi Biotec, Bergisch Gladbach, Germany), according to the manufacturer's instructions.

Cell lines

Leukaemia cell lines were obtained from the ATCC (American Type Culture Collection) or DSMZ (German Collection of Microorganisms and Cell Cultures), all cell lines were authenticated and tested for mycoplasma. Cells were cultured in Iscove's Modified Dulbecco's Medium (IMDM; Life Technologies) supplemented with 10 to 20% foetal bovine serum (FBS; Gemini Bio-Products) and 1% penicillin/streptomycin (Pen/Strep; Life Technologies). N-acetyl cysteine (NAC) was obtained from Millipore.

Analysis of CD68 Expression

Leukaemia cell lines were blocked in FACS buffer (PBS + 0.5% FBS) containing human Fc block (BD Biosciences; 564220) for 20 min at room temperature. Cells were fixed, permeabilized using the BD Cytofix/Cytoperm fixation/permeabilization kit (BD Bioscience) and later stained with anti-human CD68-PECy7 (BioLegend; 333816). Sample acquisition was performed on a BD LSR II flow cytometer and the mean fluorescence intensities (MFI) were calculated using FlowJo 9.3 software for Mac OS X (TreeStar).

Uptake and cytotoxic effect of Ferumoxytol-Cy5.5 labelled

To evaluate the cellular uptake of ferumoxytol-Cy5.5 labelled, leukaemia cell lines were seeded a density of 5 X 10^4 cells/mL. Cells were treated with ferumoxytol-Cy5.5 0.1 mg/mL and incubated at 37 °C for 6h. Afterward, cells were washed with FACS buffer and stained with DAPI 1μg/mL. Sample were evaluated by flow cytometry using a BD LSR II cytometer. The percentage of cells positive for ferumoxytol-Cy5.5 was determined relative to the vehicle control cells.

To test the effect of ferumoxytol-Cy5.5 on cell viability, cells were seeded as previously described and treated every 24h with ferumoxytol-Cy5.5 0.1 mg/mL and incubated at 37 °C. Staining with DAPI 1μg/mL and sample recording was performed at the indicated times. At least 1X10^4 events per condition were recorded on a BD LSR II flow cytometer. Cells that were negative for DAPI were scored as viable, and the viability of treated cells was normalized to control cells (PBS only). ROS-dependent cell death was determined by pre-treatment of the cells with N-acetyl-cysteine (NAC) 1mM/L for 2 hours previous to the ferumoxytol-Cy5.5 exposure. Each in vitro assay was conducted in triplicate and repeated at least three times. Cell viability is expressed on percentage in ferumoxytol-Cy5.5 treated cells relative to control cells.

Measurement of Cytosolic and Mitochondrial ROS levels

Cytosolic ROS changes were monitored using 5-(and6)chloromethyl-2',7'-dichlorodihydrofluorescein diacetate, acetyl ester (CM-H2DCFA, C6827 Invitrogen, Molecular Probes) and the Mitochondrial ROS changes were assessed using the MitoSox Red Mitochondrial superoxide indicator (MitoSox, M36008 Invitrogen, Molecular Probes). Both fluorescent dyes were prepared as a 5 mmol/L solution in DMSO and stored a −20°C. According to manufacturer's instructions, leukaemia lines were co-stained with CM-H2DCFDA and MitoSox for 30 min at 37 °C before the end of the incubation with ferumoxytol-Cy5.5 for the indicated treatment times. The fluorescence shift indicative of cytosolic or mitochondrial ROS change was analysed on a BD LSRII flow cytometer. The cytosolic or Mitochondrial ROS levels were expressed as fold change determined by calculating the fold change in ferumoxytol-Cy5.5 treated cells relative to the ROS levels in control cells.

Nanoparticles

Nanoparticles in the form of Ferumoxytol (Feraheme; AMAG pharmaceuticals, Waltham, MA, USA) were acquired from the MSKCC pharmacy. ferumoxytol doses used for *in vivo* administration were diluted from 30 mg/mL stock into sterile 0.9% NaCl bottles for dosing for a final concentration of 6mg/kg delivered in 200uL total volume. Radiolabelled version of ferumoxytol was done using the chelate free heat induced radiolabelling method[26]. Zirconium-89 (^{89}Zr) was produced on the MSKCC cyclotron and purified as zirconium oxalate. Positron emission tomography was performed on a Siemens inveon acquisition workplace v 2.0.0.1050 and inveon acquisition workstation v 4.1. Cy5.5-ferumoxytol was synthesized as previously described[30].

Oxidative ferrotherapy assessment

Peroxidase activity was performed using ferumoxytol in the presence or absence of peroxide and horseradish peroxidase. Oxidative power of ferumoxytol was determined by chemiluminescence with 1.25mg ml^{-1} luminol and titrations of ferumoxytol or iron equivalent up to 1000μg Fe per well. Radiances were measured immediately and through 30 minutes of luminol mixture addition on an IVIS Spectrum imager using an open filter (n=8 per group).

Iron determination

Intracellular iron was determined by a complete digest of the cell with iron content determined by inductively coupled plasma mass spectrometry. Iron determined was reported in mg per mg of protein determined before sample digestion by BCA.

Animal models

Syngeneic model.—C57BL/6 of 6–8 weeks old mice were purchased from Jackson Laboratories. Mice were housed in temperature and humidity-controlled animal facility with a 12-h light/dark cycle and had free access to water and food. The experimental procedures were approved by the Institutional Animal Care and Use Committee of Weill Cornell Medicine and Memorial Sloan Kettering Cancer Center. Murine bcCML was generated by the injection of spleen cells (40 $\times 10^4$ cells/mouse) carrying BCR-ABL/NUP98-HOXA9 oncogenes generously provided by Craig T. Jordan (University of Colorado School of Medicine)[19,31]. When around 0.1% of leukemic blasts were detected in PB, mice were randomly separated into the study cohorts. Animals that exceeded 2 SD from the mean % of leukemic blasts in PB were excluded from the study. Ten mice per cohort were used for survival studies to allow for 10% resolution. Mice were randomly assigned to treatment groups based upon housing cage with two cages per group. Investigators were not blinded to the therapy mice were receiving. Ferumoxytol was administered by IV (2x/week) or IP (3x/week) injection. Ara-C was administered by IP four consecutive days. The body weight and leukemic burden were monitored weekly in PB. Animals were sacrificed at the indicated time points or at signs of distress. PB, BM and SPL were harvested to evaluate leukemic burden.

Xenotransplants.—Non-obese diabetic/severe combined immunodeficient (NOD/SCID) or NOD/SCID IL2Rgamma null (NSG) mice were obtained from the Jackson Laboratories (Bar Harbor, ME, USA). Mice were sub-lethally irradiated with 200 rad using a RadSource-2000 X-ray irradiator (RadSource, BocaRaton, FL, USA) the day before transplantation. Primary AML samples or CB CD34+ cells were injected via tail vein (2–5 million cells for AML; 300K for CD34+ CB) in a final volume of 0.2 ml of FACS buffer (PBS with 0.5% FBS). After human cell engraftment was confirmed by evaluating PB (3–4 weeks) treatment with ferumoxytol (5 mg/kg; IV) was initiated. Mice were treated twice a week for 4 weeks.

Flow cytometry

Ferroportin evaluation.—For primary AML samples, cells were stained with anti-human CD45 conjugated to allophycocyanin-cyanine (APC-H7; 2D1, BD Biosciences, Franklin Lakes, NJ, USA), CD34 conjugated to phycoerythrin-cyanine-7 (PECy7; 581, BD Biosciences, Franklin Lakes, NJ, USA) and CD38 conjugated to allophycocyanin (APC; HB7, BD Biosciences, Franklin Lakes, NJ, USA) and Ferroportin (FPN) conjugated to Alexa Fluor-405 (AF-405; 8G10NB, Novus Biologicals, Littleton, CO, USA) or isotype control AF-405 (mouse IgG2b; MPC11 (Novus Biologicals, Littleton, CO, USA)) for 30 min in the dark at 4^{o}C. For cell lines, cells were only stained with FPN-AF-405 or Isotype control for 30 min in the dark at 4^{o}C. Cells were washed two times and resuspended in cold FACS buffer containing a viability dye (7-aminoactinomycin; 7AAD, Life Technologies, Carlsbad, CA, USA). Cells were evaluated in a BD-LSRII analytical flow cytometer. Analysis was later performed using FlowJo 9.3 software for Mac OS X (TreeStar, Ashland, OR).

Leukaemia burden evaluation in syngeneic model—was performed using evaluating the percentage of GFP or GFP and YFP positive cells in PB, BM or SPL. PB was processed by red blood cell (RBC) lysis, BM and SPL were harvested as previously described [18]

Leukaemia burden evaluation in xenograft model.—To assess human cell engraftment in BM was harvested at the indicated time point. Cells were stained with anti-human CD45-APCH7 (hCD45, 2D1), anti-mouse CD45-PECy5 (mCD45; 3OF11, BioLegend, San Diego, CA, USA). Human cells were determined by evaluating the percentage of hCD45+mCD45- cells. Cells were evaluated in a BD-LSRII analytical flow cytometer.

Inflammation and cytokine production.—Human cytokines IL1b IL6 and TNFα produced by human AML cell lines were determined using two cytokine detection kits (LEGENDplex™ Human Th Panel (13-plex) with V-bottom Plate (BioLegend, San Diego, CA, USA, #740722) or LEGENDplex™ Human Inflammation Panel (13-plex), BioLegend, San Diego, CA, USA, # 740118). The culture supernatants (SN) from AML cell lines were collected after 24h of ferumoxytol treatment and later evaluated via flow cytometry with the above kits.

Analysis was later performed using FlowJo 9.3 software for Mac OS X (Tree Star, Ashland, OR, USA).

Reverse Transcription-Quantitative polymerase chain reaction

Total RNA was isolated from leukemic cell lines, primary human samples or mouse tissues using Direct-zol (Zymo Research, Irvine, CA, USA) according to the manufacturer's protocol. Reverse transcription reaction was performed using the VILO SuperScript IV kit (Thermo Fisher Scientific, Waltham, MA, USA). Amplification for the genes of interest was performed using the PCR Master Mix (Thermo Fisher Scientific, Waltham, MA, USA). Triplicates samples per condition were evaluated on the StepOnePlus™ Real-Time PCR

(ABI-USA) instrument using absolute quantification settings with a sample volume of 20μL and 40 amplification cycles. Differences in gene expression levels were compared to ABL1 internal reference and represented as relative to normal BM CD34+ cells using the $2^{-\Delta\Delta Ct}$ method. ABL1 was assayed using Hs01104728_m1, SLC40A1 (FPN) was assayed using Hs00205888_m1, and HMOX1 was assayed using Hs0110250_m1. All TaqMan probes were obtained from Thermo Fisher Scientific and a complete list of probes used can be found in Supplementary Table 4.

Statistical analysis

All data are presented as means ± SEM and statistical analysis and graphs were performed using GraphPad Prism software (GraphPad Software, San Diego, CA, USA). For statistical analyses the data was analysed by one-way ANOVA followed by Tukey post-hoc test. For two groups comparisons, significance was determined with the two-tailed unpaired Student's test. Kaplan Meier curves were determined with a log-rank Mantel-Cox test. Principle component analysis was done using R-studio with R version 3.5.1.

Supplementary Material

Refer to Web version on PubMed Central for supplementary material.

Acknowledgments:

Funding: This work was supported by the following grants: National Institutes of Health (NIH) R01CA218615 and R01CA215700 (to J.G.), P30 CA08748 (to Craig Thompson, MSKCC) and R01CA172546 and R01CA102031 (to M.G.), ALSF for Childhood Cancer Research award (to C.K.), Mr. William H. and Mrs. Alice Goodwin and the Commonwealth Foundation for Cancer Research, and The Center for Experimental Therapeutics of Memorial Sloan Kettering Cancer Center (to J.G. as co-PI).

References

1. Almeida AM & Ramos F Acute myeloid leukemia in the older adults. Leuk Res Rep 6, 1–7, doi: 10.1016/j.lrr.2016.06.001 (2016). [PubMed: 27408788]
2. American Cancer Society. Cancer Facts & Figures 2018. American Cancer Society. Cancer Facts & Figures 2018 (2018).
3. Gashaw I, Ellinghaus P, Sommer A & Asadullah K What makes a good drug target? Drug discovery today 17 Suppl, S24–30, doi:10.1016/j.drudis.2011.12.008 (2012). [PubMed: 22155646]
4. Zong H et al. A Hyperactive Signalosome in Acute Myeloid Leukemia Drives Addiction to a Tumor-Specific Hsp90 Species. Cell Rep 13, 2159–2173, doi:10.1016/j.celrep.2015.10.073 (2015). [PubMed: 26628369]
5. Lapidot T et al. A cell initiating human acute myeloid leukaemia after transplantation into SCID mice. Nature 367, 645, doi:10.1038/367645a0 (1994). [PubMed: 7509044]
6. Krug U, Buchner T, Berdel WE & Muller-Tidow C The treatment of elderly patients with acute myeloid leukemia. Dtsch Ärztebl Int 108, 863–870, doi:10.3238/arztebl.2011.0863 (2011). [PubMed: 22259641]
7. Guzman ML et al. The sesquiterpene lactone parthenolide induces apoptosis of human acute myelogenous leukemia stem and progenitor cells. Blood 105, 4163–4169, doi:10.1182/blood-2004–10-4135 (2005). [PubMed: 15687234]
8. Wen J, You KR, Lee SY, Song CH & Kim DG Oxidative stress-mediated apoptosis. The anticancer effect of the sesquiterpene lactone parthenolide. J Biol Chem 277, 38954–38964, doi:10.1074/jbc.M203842200 (2002). [PubMed: 12151389]

9. Gao L et al. Intrinsic peroxidase-like activity of ferromagnetic nanoparticles. Nat Nanotechnol 2, 577–583, doi:10.1038/nnano.2007.260 (2007). [PubMed: 18654371]
10. Pinnix ZK et al. Ferroportin and Iron Regulation in Breast Cancer Progression and Prognosis. Science Translational Medicine 2, 43ra56–43ra56, doi:10.1126/scitranslmed.3001127 (2010).
11. Deng Z, Manz DH, Torti S & Torti FM Effects of ferroportin-mediated iron depletion in cells representative of different histological subtypes of prostate cancer. Antioxid Redox Signal, doi: 10.1089/ars.2017.7023 (2017).
12. Nemeth E et al. Hepcidin Regulates Cellular Iron Efflux by Binding to Ferroportin and Inducing Its Internalization. Science 306, 2090–2093, doi:10.1126/science.1104742 (2004). [PubMed: 15514116]
13. Torti SV & Torti FM Iron and cancer: more ore to be mined. Nat Rev Cancer 13, 342–355, doi: 10.1038/nrc3495 (2013). [PubMed: 23594855]
14. Basuli D et al. Iron addiction: a novel therapeutic target in ovarian cancer. Oncogene 36, 4089–4099, doi:10.1038/onc.2017.11 (2017). [PubMed: 28319068]
15. Gu Z et al. Decreased ferroportin promotes myeloma cell growth and osteoclast differentiation. Cancer research 75, 2211–2221, doi:10.1158/0008–5472.CAN-14–3804 (2015). [PubMed: 25855377]
16. Strauss WE, Dahl NV, Li Z, Lau G & Allen LF Ferumoxytol versus iron sucrose treatment: a post-hoc analysis of randomized controlled trials in patients with varying renal function and iron deficiency anemia. BMC Hematol 16, 20, doi:10.1186/s12878–016-0060-x (2016). [PubMed: 27462400]
17. Birben E, Sahiner UM, Sackesen C, Erzurum S & Kalayci O Oxidative Stress and Antioxidant Defense. The World Allergy Organization journal 5, 9–19, doi:10.1097/WOX.0b013e3182439613 (2012). [PubMed: 23268465]
18. Ashton JM et al. Gene sets identified with oncogene cooperativity analysis regulate in vivo growth and survival of leukemia stem cells. Cell Stem Cell 11, 359–372, doi:10.1016/j.stem.2012.05.024 (2012). [PubMed: 22863534]
19. Neering SJ et al. Leukemia stem cells in a genetically defined murine model of blast-crisis CML. Blood 110, 2578–2585, doi:10.1182/blood-2007–02-073031 (2007). [PubMed: 17601986]
20. Cerami E et al. The cBio cancer genomics portal: an open platform for exploring multidimensional cancer genomics data. Cancer Discov 2, 401–404, doi:10.1158/2159–8290.CD-12–0095 (2012). [PubMed: 22588877]
21. Pei S et al. Rational Design of a Parthenolide-based Drug Regimen That Selectively Eradicates Acute Myelogenous Leukemia Stem Cells. J Biol Chem 291, 21984–22000, doi:10.1074/jbc.M116.750653 (2016). [PubMed: 27573247]
22. Tesfay L et al. Hepcidin regulation in prostate and its disruption in prostate cancer. Cancer research 75, 2254–2263, doi:10.1158/0008–5472.CAN-14–2465 (2015). [PubMed: 25858146]
23. Cairns RA, Harris IS & Mak TW Regulation of cancer cell metabolism. Nature Reviews Cancer 11, 85, doi:10.1038/nrc2981 (2011). [PubMed: 21258394]
24. Prousek J Fenton chemistry in biology and medicine. Pure and Applied Chemistry 79, 2325–2338, doi:10.1351/pac200779122325 (2007).
25. Raynal I et al. Macrophage endocytosis of superparamagnetic iron oxide nanoparticles: mechanisms and comparison of ferumoxides and ferumoxtran-10. Invest Radiol 39, 56–63, doi: 10.1097/01.rli.0000101027.57021.28 (2004). [PubMed: 14701989]
26. Boros E, Bowen AM, Josephson L, Vasdev N & Holland JP Chelate-free metal ion binding and heat-induced radiolabeling of iron oxide nanoparticles. Chemical Science 6, 225–236, doi: 10.1039/c4sc02778g (2015). [PubMed: 28553472]
27. Cheson B et al. National Cancer Institute-sponsored Working Group guidelines for chronic lymphocytic leukemia: revised guidelines for diagnosis and treatment. Blood 87, 4990–4997 (1996). [PubMed: 8652811]
28. Zanganeh S et al. Iron oxide nanoparticles inhibit tumour growth by inducing pro-inflammatory macrophage polarization in tumour tissues. Nat Nanotechnol 11, 986–994, doi:10.1038/nnano.2016.168 (2016). [PubMed: 27668795]

29. Auerbach M, Chertow GM & Rosner M Ferumoxytol for the treatment of iron deficiency anemia. Expert Review of Hematology 11, 829–834, doi:10.1080/17474086.2018.1518712 (2018). [PubMed: 30188740]

30. Yuan H et al. Heat-induced radiolabeling and fluorescence labeling of Feraheme nanoparticles for PET/SPECT imaging and flow cytometry. Nat Protoc 13, 392–412, doi:10.1038/nprot.2017.133 (2018). [PubMed: 29370158]

31. Huntly BJ et al. MOZ-TIF2, but not BCR-ABL, confers properties of leukemic stem cells to committed murine hematopoietic progenitors. Cancer Cell 6, 587–596, doi:10.1016/j.ccr.2004.10.015 (2004). [PubMed: 15607963]

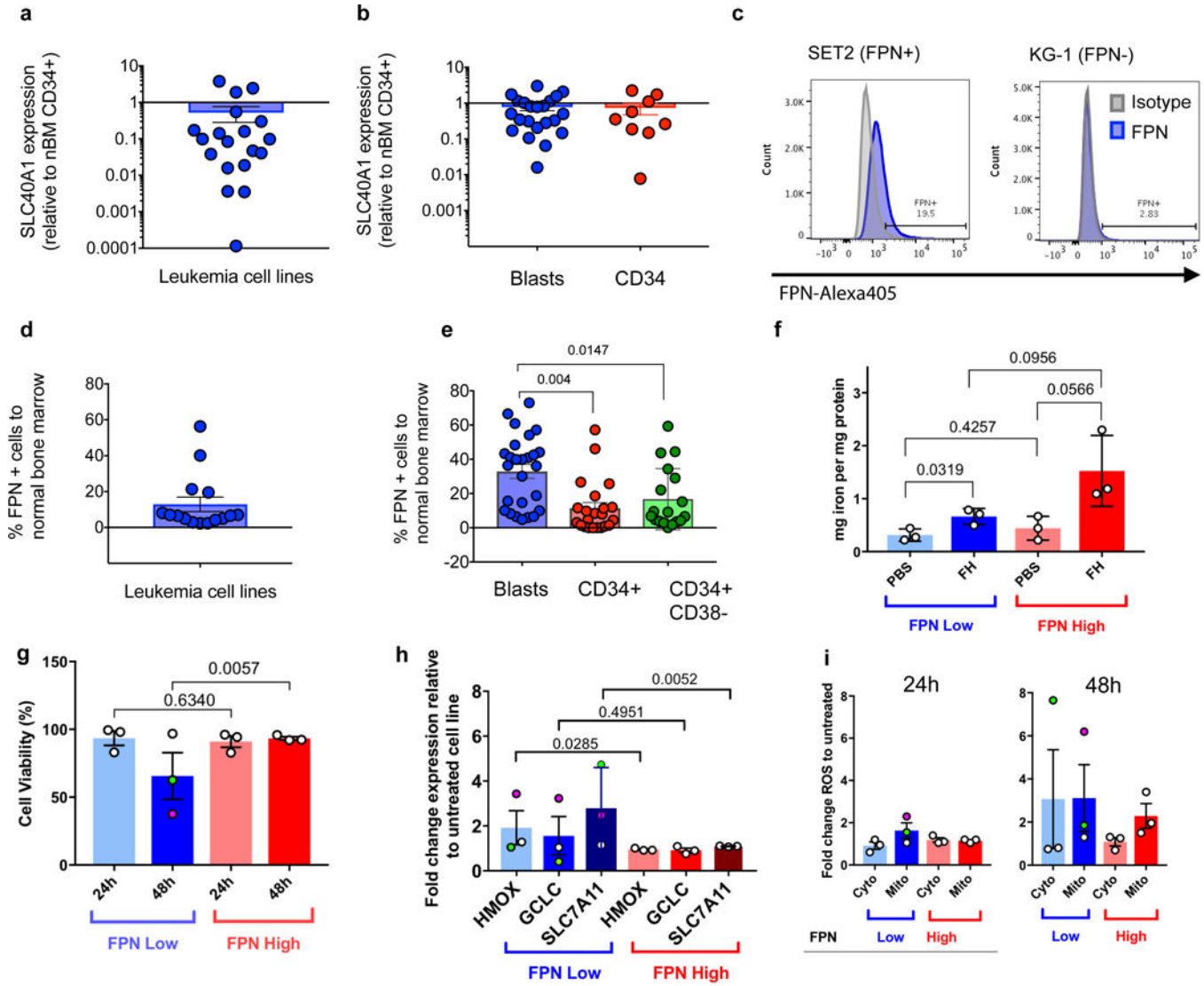

Figure 1. Reduced expression of FPN is a feature of leukaemia cell lines and primary AML samples.

SLC40A1 (FPN) transcript expression relative to normal bone marrow CD34+ progenitor cells (nBM CD34+) in (**A**) leukaemia cell lines (n=19 cell lines) and (**B**) primary AML samples (n=31 AML samples), blasts and CD34+ are shown. **(C)** Representative example of the flow cytometry analysis for FPN expression in cell lines, n = 20 cell lines measured and reported in Supplementary Table 1. **(D)** Percent expression of FPN using flow cytometry in cell lines (n=19 cell lines), and (**E**) primary AML samples (n=31 AML samples) in the indicated populations. Human AML cell lines stratified by FPN expression relative nBM CD34+ cells, are represented as low (blue) and high (red) to evaluate (**F)** iron content at 24h (n=3 cell lines for FPN-low and FPN-high) determined by ICP-MS and **(G)** cell survival, represented by cell counts at 24h and 48 h after exposure to ferumoxytol (FH) or PBS (n=3 per group and timepoint). Green and pink dot represents KCL22 and MV411 respectively through panels g-i. (**H**) Levels of gene expression for HMOX1, GCLC, and SLC7A11 relative to untreated samples (n=3 technical replicates per cell line, n=3 cell lines (shown

with SEM) for FPN-low and FPN-high lines (n=6 cell lines total). (**I**) Cytosolic and mitochondrial staining for ROS using H_2DCFDA and MitoSox, respectively reveal elevated ROS levels in FPN-low lines (n=2 independent measurements per cell line (n=3 cell lines per FPN low or FPN high group) per timepoint). SEM determined based on cell lines in each FPN low or high group as biological replicates). Each symbol represents a sample, bar represents the mean and the error bar represents the SEM. An ordinary one-way ANOVA was used for Fig. 1e. A two-tailed unpaired t-test was used for Figs. 1f-h. Flow experiments were performed one time with corresponding controls (unstained, isotype, or FMO). RT-PCR data was also performed once with each cell line and gene in triplicate.

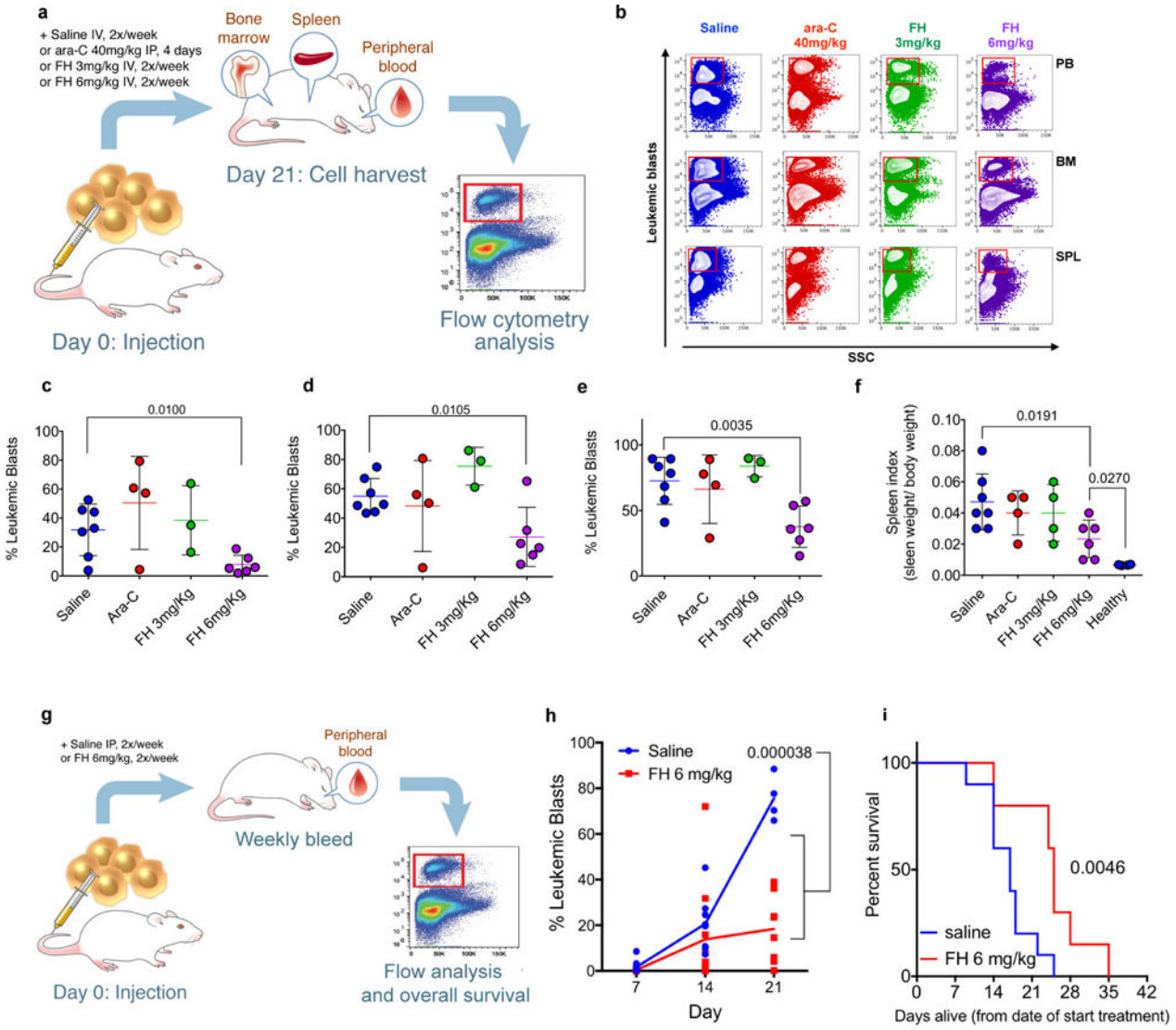

Figure 2. ***In vivo*** **treatment of mice having blast crisis CML with ferumoxytol reduces leukaemia burden and improves overall survival.**

(a) Schematic representation for the experimental plan to evaluate anti-leukaemia activity *in vivo* using the murine blast crisis CML model (bcCML). **(b)** Representative flow cytometry panel showing leukemic blasts (red boxes) in peripheral blood (PB), bone marrow (BM), and spleen (SPL) after the treatment with saline (blue, n=7 mice), Ara-C (red, n=4 mice), ferumoxytol 3 mg/kg (green, n=3 mice), ferumoxytol (FH) 6 mg/kg (purple, n=6 mice) flow analysis was performed once on the samples with controls (unstained, isotype, or FMO) present and samples run in triplicate. Scatter plots for the percent leukemic blasts for all animals from the indicated cohorts in PB (**c**), BM (**d**), and SPL (**e**). Each symbol represents an individual mouse. Bar represents the mean; error bar represents the SEM. (**f**) Spleen index (spleen weight normalized to body weight). (**g**) Schematic representation for the experimental plan to evaluate the effect of ferumoxytol in overall survival. (**h**) Percent leukemic blasts in PB at the indicated time points. Each point represents an individual surviving mouse with the average represented as the solid line. Day 7: saline n=10 mice,

ferumoxytol n=10 mice; day 14: saline n=7 mice, ferumoxytol n=10 mice; day 21: saline n=3 mice, ferumoxytol n=8 mice). Experiment performed one time. (**i**) Kaplan-Meier survival plot for mice treated with saline or ferumoxytol (n=10 mice per group). Data are shown as mean ± SEM. Unpaired two-tailed t-tests were used to compare between saline and ferumoxytol 6mg kg^{-1} in Fig. 2c-f. Experiment performed twice and replicate curve reported in Supplementary Fig. 13. Multiple t-tests for 7, 14, and 21 days assuming different SDs were used for Fig. 2h with a false discovery rate of 5% using a two-stage set-up method. Comparison of survival curves in Fig. 2i was performed using a log-rank Mantel-Cox test.

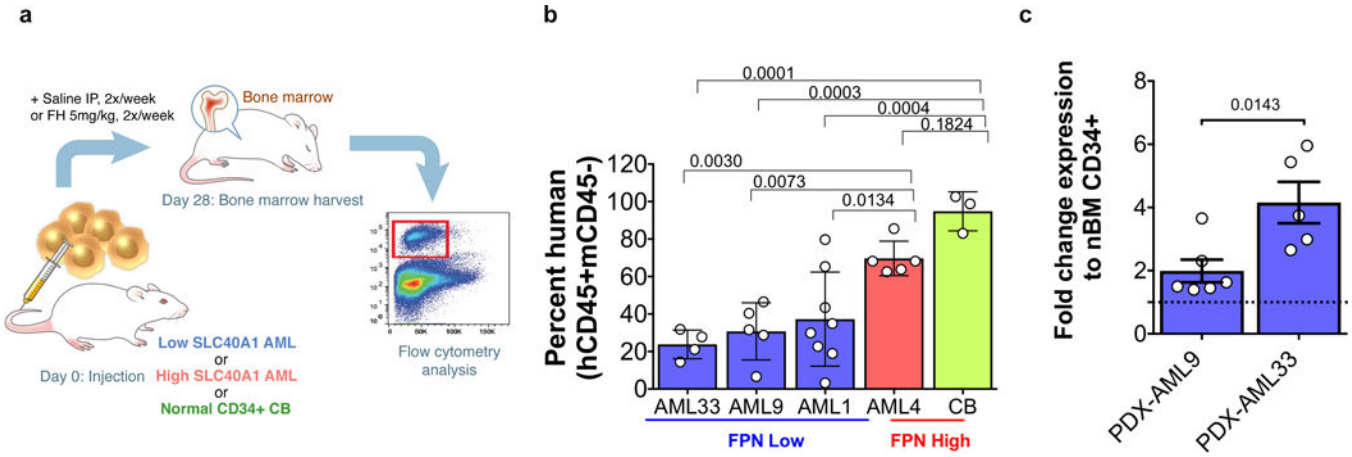

Figure 3. Ferumoxytol treatment targets leukaemia cells from patient derived xenografts (PDX) from primary AML samples with low FPN without harming normal cells.

(a) Schematic representation for the experimental plan to evaluate anti-leukaemia activity *in vivo* using PDX mice from primary AML samples with low or high FPN, xenografts were also established using normal CD34+ cells from cord blood (CB). **(b)** Percent human cell engraftment relative to saline-treated control for mice treated with 5 mg/kg ferumoxytol (FH) for 4 weeks. FPN (SLC40A1) low samples (blue, n=4) AML33, AML9 (n=5), and AML1 (n=8), FPN (SLC40A1) high sample (red, n=5) AML4 and CB (grey, n=3) are shown. Each symbol represents an individual mouse, bars represent the mean, error bar represents the SEM. **(c)** Fold change expression in transcriptional levels of HMOX1 relative to normal bone marrow CD34+ after treatment with ferumoxytol (n=6 mice AML9, n=5 mice AML 33). Data are shown as mean ± SEM and analysis was done using an ordinary one-way ANOVA for Fig. 3b while a two-tailed unpaired t-test was used in Fig. 3c. AML-PDX experiment performed once due to sample availability.

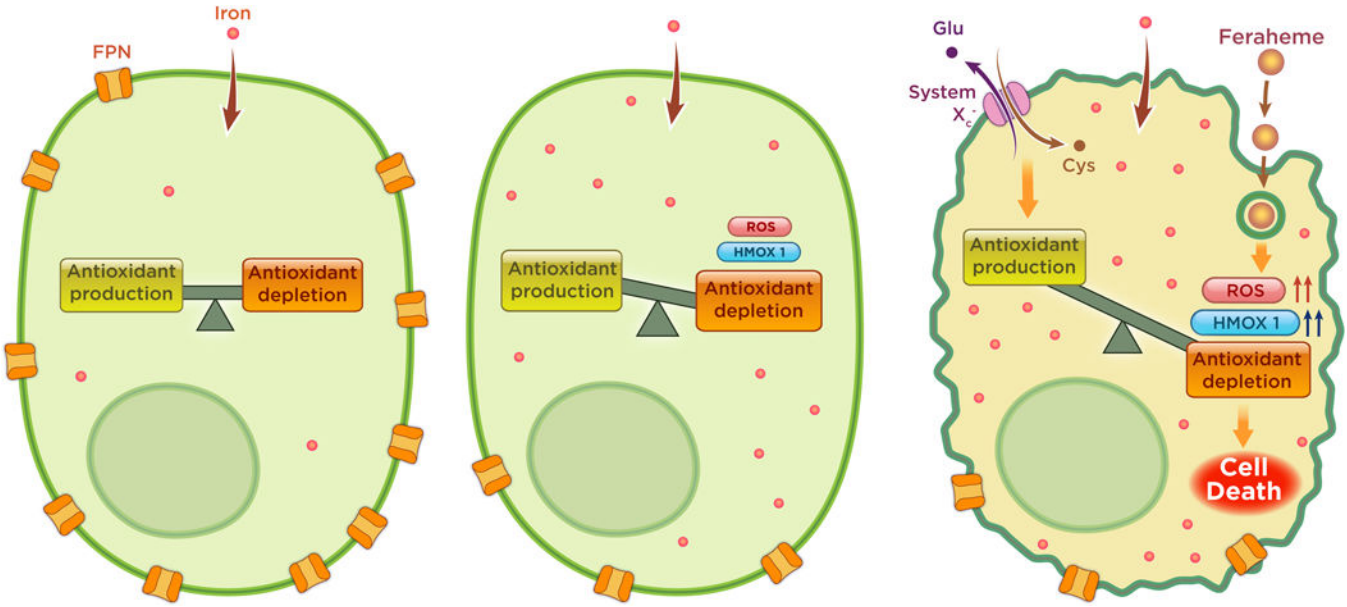

Figure 4. Oxidative Ferrotherapy through low ferroportin expression in leukaemia cells.

Normal cells (left) maintain a sufficiently high expression of FPN that allow cells to digest and transport iron without damaging effects of ROS from Fenton chemistry. Leukemic cells, including LSCs, in contrast that contain abnormally low expression of FPN (middle) will allow the accumulation of iron and cellular stress due to increased ROS. Upon addition of ferumoxytol (FH) (Right), AML cells low in FPN are increasingly stressed, overcoming antioxidant production, resulting in cell death.